Journal of Hazardous Materials 217–218 (2012) 439–446

Contents lists available at SciVerse ScienceDirect

Journal of Hazardous Materials

journal homepage: www.elsevier.com/locate/jhazmat

# Superparamagnetic high-surface-area $Fe_3O_4$ nanoparticles as adsorbents for arsenic removal

Liyun Feng[a,b], Minhua Cao[a,*], Xiaoyu Ma[a], Yongshuang Zhu[a], Changwen Hu[a,*]

[a] Key Laboratory of Cluster Science, Ministry of Education of China, Department of Chemistry, Beijing Institute of Technology, Beijing 100081, PR China
[b] Center of Analysis and Testing, Beihua University, Jilin 132013, PR China

ARTICLE INFO

*Article history:*
Received 21 October 2011
Received in revised form 25 March 2012
Accepted 26 March 2012
Available online 3 April 2012

*Keywords:*
$Fe_3O_4$
Superparamagnetic
Nanoparticles
Adsorbents
Arsenic removal

ABSTRACT

Superparamagnetic ascorbic acid-coated $Fe_3O_4$ nanoparticles with a high specific surface area were successfully synthesized via an environmentally friendly hydrothermal route in the absence of any templates. The as-synthesized ascorbic acid-coated $Fe_3O_4$ nanoparticles have a diameter of less than 10 nm, thus leading to a high specific surface area of about 179 $m^2/g$, which is even larger than those of well-defined mesoporous structures. The only used capped agent is ascorbic acid, which serves as a functionalized molecule to make sure the high dispersibility and stability of the ascorbic acid-coated $Fe_3O_4$ nanoparticles in aqueous solution. The ascorbic acid-coated $Fe_3O_4$ nanoparticles exhibit superparamagnetic properties at room temperature and saturation magnetization approaches 40 emu $g^{-1}$. The ascorbic acid-coated $Fe_3O_4$ nanoparticles were evaluated as an absorbent to remove heavy metal arsenic from wastewater. The adsorption data obeyed the Langmuir equation with a maximum adsorption capacity of 16.56 mg/g for arsenic (V), and 46.06 mg/g for arsenic (III).



## 1. Introduction

The removal of arsenic (As) from natural waters has attracted considerable attention because of its toxicity to environment and human health. As well known, the most commonly existing forms of arsenic species in aqueous environments are arsenate (as $H_2AsO_4^-$ and $HAsO_4^{2-}$) in well-oxidized waters and arsenite (as $H_3AsO_3^0$ and $H_2AsO_3^-$) in reduced environments [1,2], while arsenite is 25–60 times more toxic than arsenate and more mobile in the environment [3]. Arsenic is known to easily deposit in certain organs by drinking arsenic-laden water and consuming crops grown from arsenic-accumulated soils, respectively, including the skin, liver, lung, and kidney, a pattern compatible with arsenic-associated cancer in these organs. Therefore, it is really necessary to remove arsenic from water to make sure that our environment is safe. Recently, it has been reported that $Fe_3O_4$-based materials are very effective in the removal of arsenic (arsenate and arsenite) due to their strong adsorption activities and the properties of being easily separated, collected and reused by an external magnetic field [4–6]. The removal of adsorbents from solution with the use of magnetic field is more selective and efficient than centrifugation or filtration. In the recent years, $Fe_3O_4$ nanoparticles have attracted increasing research attentions in the field of environment protection and remediation because of their unique properties described above [7–11]. However, these adsorbents are difficult to recycle, since $Fe_3O_4$ is highly susceptible to oxidation because of its small size when exposed to the atmosphere [4,12]. To overcome this drawback, the surface functionality of $Fe_3O_4$ nanoparticles was achieved by some researchers. For example, $Fe_3O_4$ nanoparticles modified with an oleic acid ligand exhibit an improved uptake for capturing arsenic (III) and arsenic (V) [6]; thiol functionalized superparamagnetic $Fe_3O_4$ nanoparticles exhibited effective removal of toxic soft metals such as Hg, Ag, Pb, Cd, and Tl from aqueous systems [7]; chitosan coated $Fe_3O_4$ nanoparticles could be used as a magnetic nano-adsorbent for the removal of heavy metal ions such as Cu(II) [8]; humic acid (HA) coated $Fe_3O_4$ nanoparticles ($Fe_3O_4$/HA) were developed for the removal of toxic Hg(II), Pb(II), Cd(II), and Cu(II) from water [9].

To ensure high adsorption performance of $Fe_3O_4$ nanoparticles, high surface area and dispersibility are quite necessary because these two factors can improve interfacial interaction between adsorbents and heavy metal ions. Recently, several methods have been developed to fabricate porous $Fe_3O_4$ nanostructures in order to obtain high surface area. However, no desirable results are reported. Thermal decomposition of the iron precursor in organic solution is the most commonly used synthetic route. But organic phase reaction generally suffers from not only toxic organic solvent, high-cost, hardly washing surfactant, or a high reaction temperature of 400 °C [13], but also the formation of some byproducts, such as ferrihydrite ($Fe_5HO_8{\cdot}4H_2O$), akagenite (β-FeOOH), $Fe(OH_3)$,

* Corresponding authors. Tel.: +86 10 68912631; fax: +86 10 68912631.
*E-mail address:* caomh@bit.edu.cn (M. Cao).

0304-3894/$ – see front matter © 2012 Elsevier B.V. All rights reserved.
http://dx.doi.org/10.1016/j.jhazmat.2012.03.073

etc. Thus, the final product usually is a mixture of two or three phases, thus limiting their direct application in water systems [14]. Therefore, it is still challenging to develop a simple, low-cost, and environmentally friendly green route for synthesizing high-surface-area $Fe_3O_4$ nanoparticles with high water dispersibility.

Here, we present a simple green route for synthesizing high-surface-area ascorbic acid-coated $Fe_3O_4$ nanoparticles under hydrothermal conditions by using $FeCl_3{\cdot}6H_2O$, $N_2H_4{\cdot}H_2O$, and ascorbic acid (Vc) as precursors. The as-synthesized ascorbic acid-coated $Fe_3O_4$ nanoparticles exhibit high water solubility. More importantly, they possess a lager surface area of 179 $m^2/g$, which is the first report of $Fe_3O_4$ nanomaterials with such a high surface area to date. The ascorbic acid-coated $Fe_3O_4$ nanoparticles exhibit superparamagnetic properties at room temperature and saturation magnetization approaches 40 emu $g^{-1}$. They were evaluated as an absorbent to remove heavy metal arsenic from wastewater. The maximum adsorption occurred at pH = 7 with values of 16.56 mg/g for arsenic (V), and 46.06 mg/g for arsenic (III) when initial arsenic concentration was kept at 1 mg/L.

## 2. Experimental

### 2.1. Synthesis of ascorbic acid-coated $Fe_3O_4$ nanoparticles

All chemicals used were analytical grade without further purification. In a typical synthesis, 1 mmol of $FeCl_3{\cdot}6H_2O$ was dissolved in 40 mL distilled water under vigorous magnetic stirring to form a clear solution, followed by the addition of 3 mmol of ascorbic acid and 5 mL of $N_2H_4{\cdot}H_2O$ (50% v/v). Then the solution was transferred into 60 mL Teflon-line stainless steel autoclave, heated at 180 °C in an electric oven for 8 h, and then cooled to room temperature naturally. The precipitate was collected by centrifugation and washed with deionized water and absolute ethanol several times and dried under vacuum at 60 °C for 6 h.

### 2.2. Characterizations

The size and morphology were observed by transmission electron microscope (TEM) and high resolution TEM (HRTEM) on a JEOL JEM-2010F at an acceleration voltage of 200 kV. Sample was prepared by placing a dilute particle suspension onto 400 mesh carbon grids coated with Formvar film. The crystalline structure of the product was characterized by a Rigaku/Dmax2000 diffractometer with Cu Kα radiation (λ = 1.5418 Å) and the scan step was 0.02 in 2θ. Raman spectroscopy was carried out using a Renishaw inVia Raman spectrometer equipped with a Leica microscope and a 633 nm laser. A drop of the colloid suspension was placed on a quartz slide and allowed to dry before raman scattering measurements. The laser power was set at 2 mW at the exit of the microscope objective. Fourier transform infrared (FTIR) spectrum was measured on a Bruker tensor 27, spectrometer from 4000 to 400 $cm^{-1}$, and the KBr disk method was employed. Magnetic measurement was carried out on a quantum Design MPMS-XL5 SQUID magnetometer with the filed sweeping from −60000 to 60000 Oe at room temperature. Zeta potential was carried out on Zetasizer Nano Series (ZS90). The Brunauer–Emmett–Teller (BET) surface area was measured on a Micromeritics ASAP 2010 analyzer. The hydrodynamic size of particles in water was measured using a Brookhaven 90 plus particle size analyzer. Inductively-coupled plasma spectrometer (ICP) was carried out on Jarrel-ASH (ICAP-9000).

### 2.3. Heavy metal absorption tests

Arsenic is considered as highly toxic pollutant in water resources and their efficient removal from water is of great importance. To evaluate the absorption ability of our sample, heavy metal absorption tests were carried out. $NaAsO_2$ and $NaAsO_4{\cdot}12H_2O$ were used as the sources of As (III) and As (V), respectively, and the pH values of the solution were adjusted using NaOH or HCl. In a typical removal procedure, ascorbic acid-coated $Fe_3O_4$ nanoparticles were added into 25 mL of As(III) solution (0.10 mg/L), sealed and shaken for 24 h with 60 rpm at room temperature. After shaking, the mixtures were placed under an external magnetic field and $Fe_3O_4$ sample was separated from solution. Arsenic concentration in the supernatant solution was measured, by using inductively coupled plasma atomic emission spectroscopy (ICP-AES). Every experiment was performed in triplicate and average values were used in the graph. The minimum detection limit of ICP-AES for arsenic was 0.003 mg/L. The adsorption capacity was roughly estimated by equation 1 as follows:

$$q_e = \frac{(C_0 - C)V}{W} \quad (1)$$

where $q_e$ (mg/g) is the adsorption capacity, $C_0$ (mg/L) is the initial concentration of the arsenic solution, $C$ (mg/L) is the equilibrium concentration of arsenic ions, $V$ (L) is the initial volume of the arsenic solution, and $W$ (g) is the weight of the adsorbent.

## 3. Results and discussion

### 3.1. Composition, size and morphology

In our experiments, ascorbic acid was used as a ligand. The advantages of the ascorbic acid are its water solubility in aqueous solution and strong coordination ability with transition metals. Fig. 1a shows the XRD pattern of the sample obtained with 3 mmol of ascorbic acid. The diffraction peaks at $2\theta = 30.1°$, 35.3°, 43.0°, 57.2°, and 62.6° match well with those from the JDPCS card (19-0629) for magnetite, and without indication of other crystalline byproducts. The average particle diameter can be estimated using Scherer's formula [15] to be about 5 nm by using the strongest peak (3 1 1) at $2\theta = 35.3°$. To exactly determine that the sample is $Fe_3O_4$, not γ-$Fe_2O_3$, Raman spectrum has to be used as an alternative tool for distinguishing the different structural phases of iron oxides. Fig. 1b depicts the Raman spectrum of the sample at room temperature. The peak at 668 $cm^{-1}$ was observed, which is typical characteristic of $Fe_3O_4$, while for γ-$Fe_2O_3$, three strong peaks at 695, 500, and 352 $cm^{-1}$ are generally found [16]. Therefore, both the XRD pattern and Raman spectrum confirmed that the composition of the sample is $Fe_3O_4$, not γ-$Fe_2O_3$.

The morphology and microstructure of the as-synthesized $Fe_3O_4$ sample were investigated by transmission electron microscopy (TEM). As shown in Fig. 2a, the sample consists of small nanoparticles with relatively uniform size and shape. The average size of the particles is about 5 nm. The high-resolution transmission electron microscopy (HRTEM) is presented in Fig. 2b, which clearly shows that the product is highly crystalline despite the small particle size. The typical lattice fringe spacing, determined to be 0.296 nm, corresponds to the spacing of the (2 2 0) planes of $Fe_3O_4$.

To highlight the effect of the ascorbic acid on the shape and size of the $Fe_3O_4$ sample, a series of controllable experiments were carried out, in which we only change the amount of the ascorbic acid while other reaction parameters were kept constant, same as those in experimental section described above. Fig. 3 shows the XRD patterns and TEM images of the samples obtained with different amounts of the ascorbic acid. It is found that without ascorbic acid, $Fe_3O_4$ phase is still obtained (Fig. 3a), but the particles are irregular and nonuniform (Fig. 3b). When the amount of ascorbic acid was increased to 1 and 2 mmol, respectively, the size of the as-resulted particles (Fig. 3c and d) remarkably decreases compared with the case of no ascorbic acid and distinct

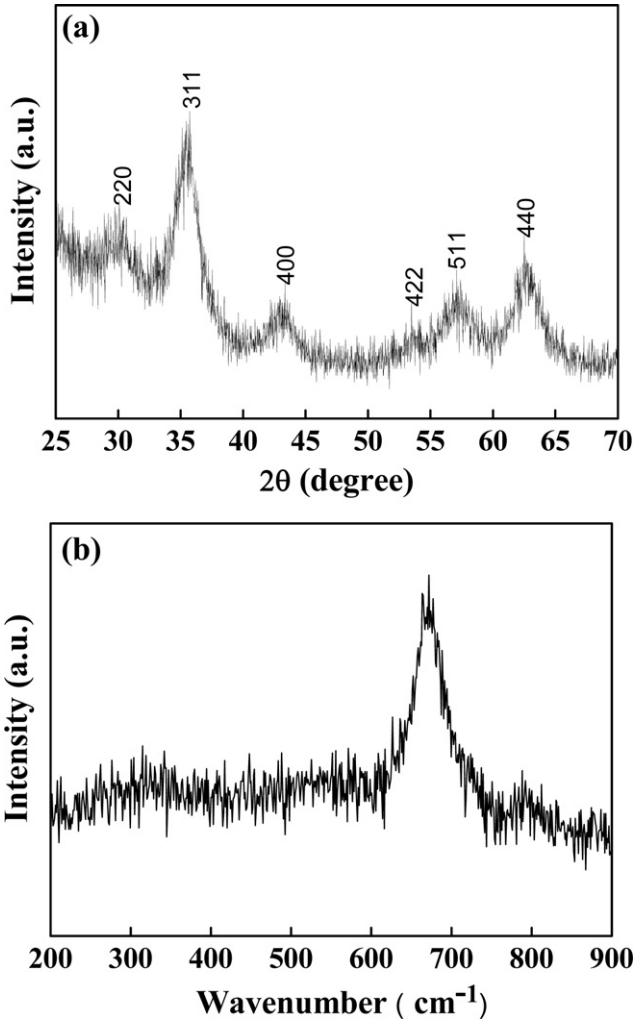


**Fig. 1.** (a) XRD pattern and (b) Raman spectrum of the as-prepared ascorbic acid-coated $Fe_3O_4$ nanoparticles.

aggregation was observed for both cases. In addition, the size of the particles for the 2 mmol of ascorbic acid is smaller than that for the 1 mmol ascorbic acid, which could also be further confirmed by XRD patterns (Fig. 3a). When the amount of ascorbic acid was increased to 3 mmol, namely, the optimum synthesized condition,

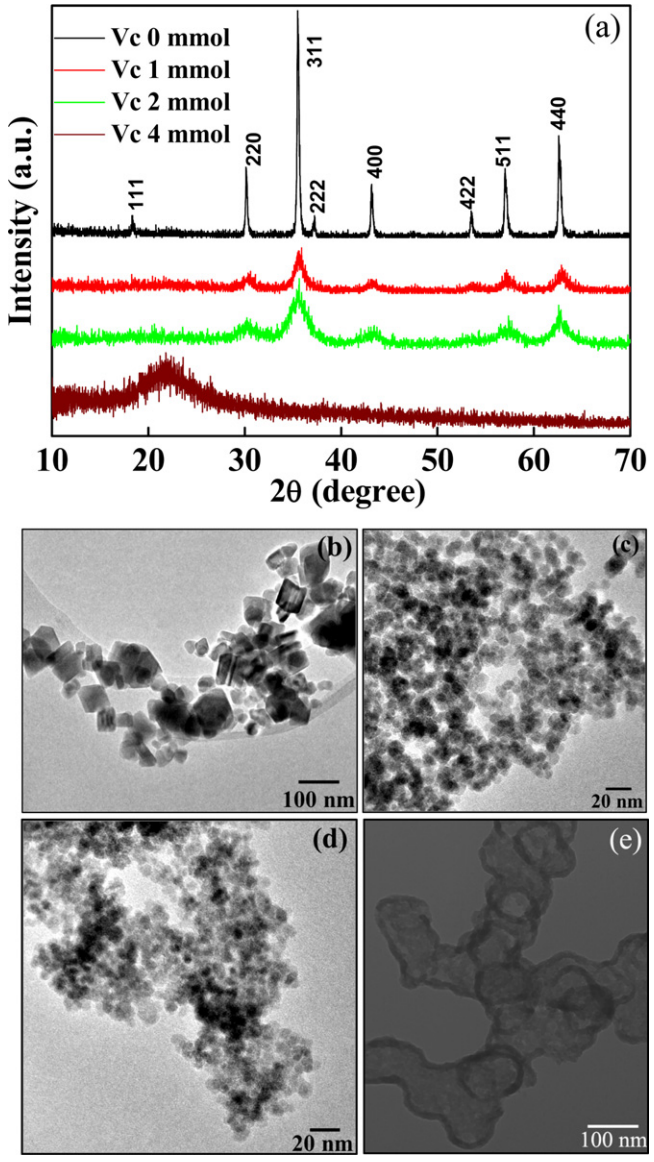


**Fig. 3.** (a) XRD patterns of the products with different Vc amounts, TEM images of the products with different Vc amounts (b) 0, (c) 1 mmol, (d) 2 mmol.

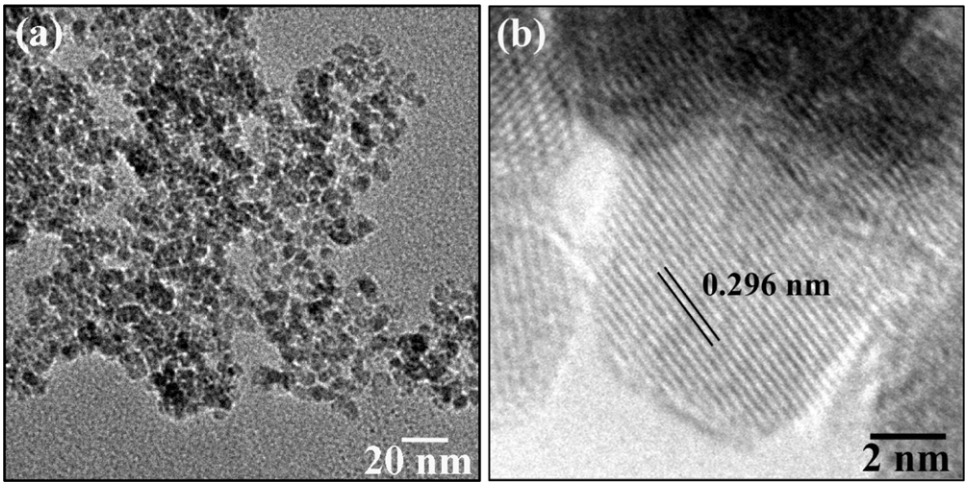


**Fig. 2.** (a) TEM and (b) HRTEM images of the as-prepared ascorbic acid-coated $Fe_3O_4$ nanoparticles.

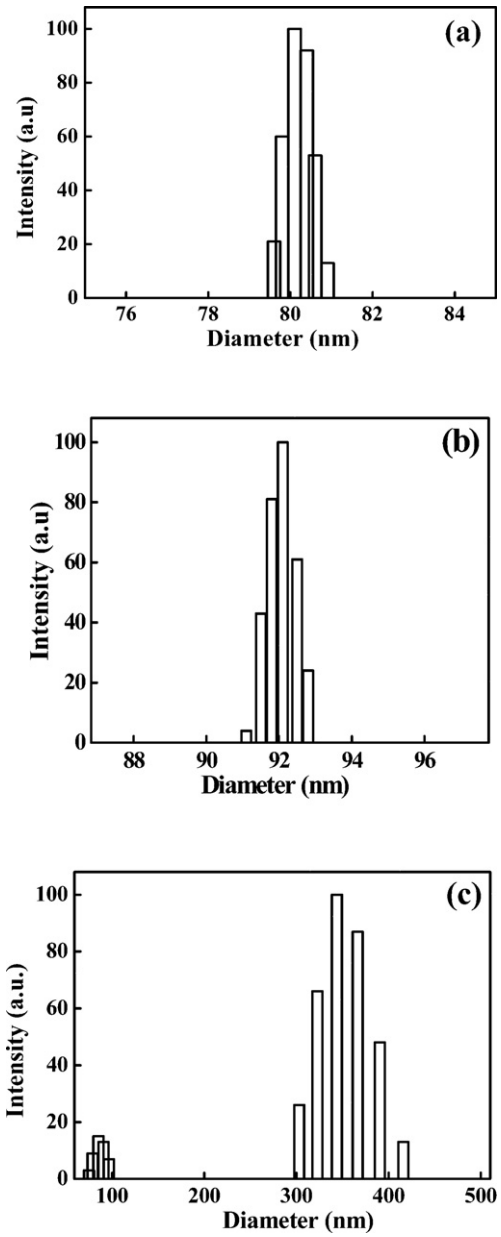


**Fig. 4.** DLS plots of the ascorbic acid-coated $Fe_3O_4$ nanoparticles with different Vc amounts (a) 3 mmol, (b) 2 mmol, (c) 1 mmol.

monodisperse and uniform nanoparticles were detected, as presented in Fig. 2a. For all samples obtained with the ascorbic acid, the diffraction peaks are clearly wider than those for the case without the ascorbic acid. Further increase in the amount of ascorbic acid (4 mmol) leads to the formation of hollow and amorphous nanostructures, as shown in Fig. 3a and e. The reason for this behavior is not yet clear and further investigation is ongoing.

In order to understand the dispersability of the nanoparticles in water, we have measured the dynamic light scattering (DLS) of the nanoparticles. As shown in Fig. 4, the nanoparticles with 3 mmol of ascorbic acid have an average size of 80.2 nm. Combining with the result of TEM, the nanoparticles have slight aggregation. When the amount of ascorbic acid decreased to 2 and 1 mmol, the average diameter of the nanoparticles increased to 92.1 and 319 nm, respectively. Especially for the case of 1 mmol of ascorbic acid, the nanoparticles also have a wider range of hydrodynamic size (75–416 nm). These results clearly demonstrate that coating $Fe_3O_4$ nanoparticles with ascorbic acid could efficiently reduce their aggregation. In addition, the nanoparticles obtained with 3 and 2 mmol of ascorbic acid both have a same polydispersity index of 0.005, while that with 1 mmol of ascorbic acid has a larger polydispersity index of 0.205, indicating that when the amount of ascorbic acid used is larger than 2 mmol, the obtained particles have a good dispersity in water.

Above results clearly show that the presence of ascorbic acid is beneficial to obtain small size nanoparticles and the amount of ascorbic acid used has an important effect on the crystallization and size of the final product. To further understand the role of ascorbic acid in the formation of small size $Fe_3O_4$ nanoparticles, the Fourier transform infrared (FT-IR) spectrum was used to characterize the surface structure of the $Fe_3O_4$ nanoparticles. For comparison, FT-IR spectrum of the ascorbic acid was also carried out, as shown in Fig. 5a. The $Fe_3O_4$ nanoparticle sample as well as ascorbic acid feature bands in the range of 3160–3430 $cm^{-1}$, assignable to the O–H vibration, the bands at 2943 and 2976 $cm^{-1}$ to C–H stretching vibration, the bands at 2835 and 1476 $cm^{-1}$ to $CH_2$ stretching modes, and the one at 1602 $cm^{-1}$ to C=O stretching vibrations. For the $Fe_3O_4$ nanoparticle sample, the band at 580 $cm^{-1}$ is typical characteristic for Fe–O [17,18]. However, the presence of two strong bands at 1024 and 1091 $cm^{-1}$, assignable to C–O–C symmetric stretching mode, and the absence of the band at 1651 $cm^{-1}$, assignable to C=C stretching vibration mode, point to the fact that ascorbic acid is probably oxidized to dehydroascorbic acid under basic conditions (Fig. 5b). This redox reaction may occur between ascorbic acid and $Fe^{3+}$, which has been reported before [19]. In our experiments, when ascorbic acid was added to yellow $FeCl_3$ aqueous solution, the color of $FeCl_3$ aqueous solution changed immediately from yellow to colorless, indicating the formation of Fe-ascorbic acid coordination compound (Fig. 5c). When this compound was treated under hydrothermal condition, $Fe_3O_4$ nanoparticles were obtained, accompanied by the oxidation of the ascorbic acid into dehydroascorbic acid. The multiple hydroxyl groups of dehydroascorbic acid chelate with the Fe atoms of $Fe_3O_4$ as a coating agent to form steric hindrance, similar to the conventional surfactants and stabilizers [20,21], thus resulting in the formation of monodisperse nanoparticles. It is interesting to note that the obtained $Fe_3O_4$ nanoparticles can be easily dispersed in water to form transparent colloids, which can be ascribed to the abundant hydrophilic groups surrounding the nanoparticles (Fig. 5d). In addition, the $Fe_3O_4$ nanoparticles could be easily separated from the solution by a magnet (Fig. 5d).

### 3.2. Magnetic properties

The magnetic properties of the ascorbic acid-coated $Fe_3O_4$ nanoparticles were investigated at room temperature. Fig. 6 shows the magnetic hysteresis curves measured at 300 K, with the field sweeping from −60 000 to 60 000 Oe. It can be seen that the sample exhibits a superparamagenetic characteristics and saturation magnetization is 40 emu $g^{-1}$, which is higher than those of similar sized $Fe_3O_4$ nanparticles prepared by the liquid–solid–solid synthetic route [14] ($D$ = 5 nm, $M_s$ = 14.6 emu $g^{-1}$) or reflux method [18,22] ($D$ = 4 nm, $M_s$ = 18 and 3 emu $g^{-1}$), and the standard hydrothermal method [21,23] ($D \approx 4$ nm, $M_s$ = 16.43 and 14.82 emu $g^{-1}$). Apart from the particle size and crystallinity, there are many factors such as surface spin-canting, surface disorder, surface ligands, cation site distribution, and stoichiometry deviation that affect the magnetic properties of nanoparticles, even when synthesized by the same approach [24,25]. Thus it can be seen that the ascorbic acid-coated $Fe_3O_4$ nanoparticles obtained by this synthesis route used here possess a high saturation magnetization. This feature is beneficial for their application in adsorption as adsorbents.

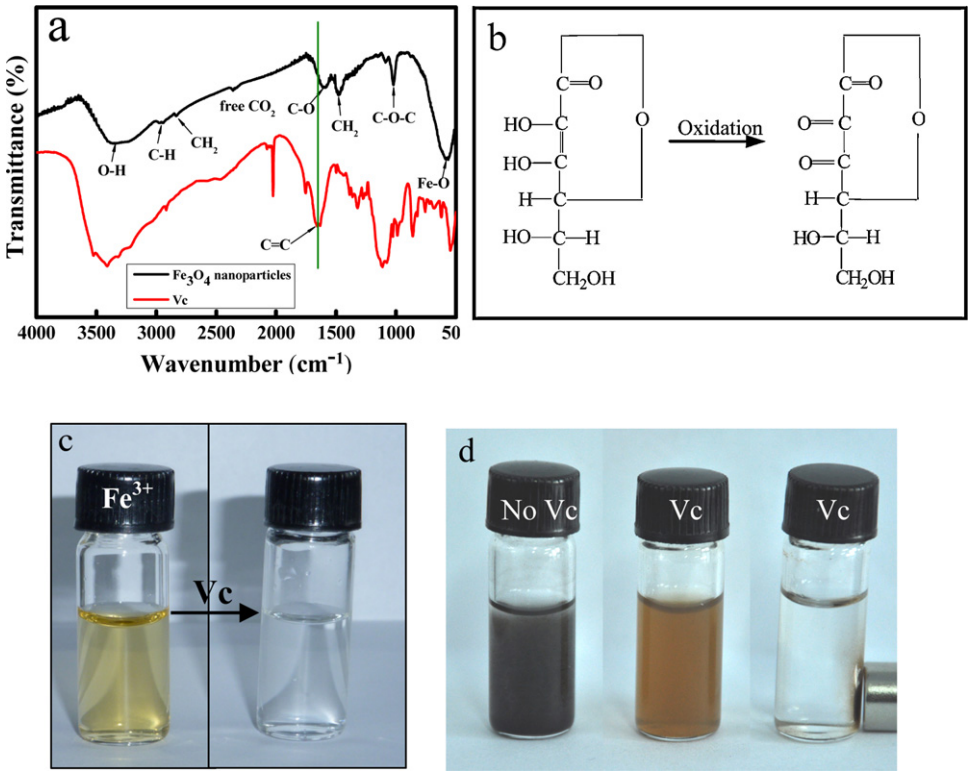


**Fig. 5.** (a) FT-IR spectra of the ascorbic acid-coated $Fe_3O_4$ nanoparticles (black line) and Vc (red line). (b) Proposed oxidation process of the Vc, (c) the photos of $FeCl_3$ aqueous solution before and after Vc addition, (d) photos of the dispersiveness of ascorbic acid-coated $Fe_3O_4$ nanoparticles and $Fe_3O_4$ sample obtained without Vc in aqueous solution.

### 3.3. Heavy metal absorption experiment

Before adsorption experiments are performed, we first measured the Brunauer–Emmett–Teller (BET) surface area of the ascorbic acid-coated $Fe_3O_4$ nanoparticles, which is an important factor that affects the behavior of a sorbent. For comparison, that of $Fe_3O_4$ particles obtained without ascorbic acid has also been measured. The BET surface area of the ascorbic acid-coated $Fe_3O_4$ nanoparticle powder is 178.48 $m^2/g$, which is much higher than that of $Fe_3O_4$ sample obtained without ascorbic acid (15.63 $m^2/g$). This value is even larger than that of $Fe_3O_4$/graphene composites [4]. The relatively large surface area is beneficial for the adsorption of harmful or toxic molecules if the ascorbic acid-coated $Fe_3O_4$ nanoparticles are used as an adsorbent. Second, we investigated the surface electrical characteristic of the ascorbic acid-coated $Fe_3O_4$ nanoparticles in water by zeta potential measurement, since zeta

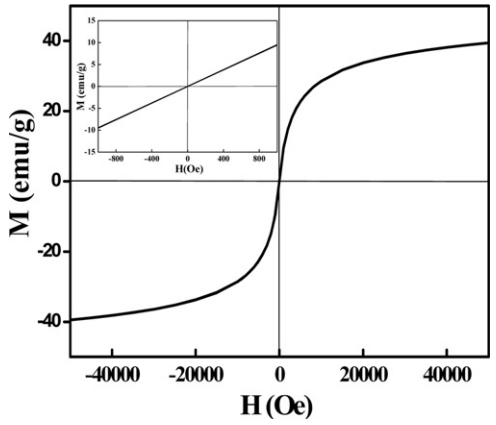


**Fig. 6.** Magnetization curves of $Fe_3O_4$ nanoparticles.

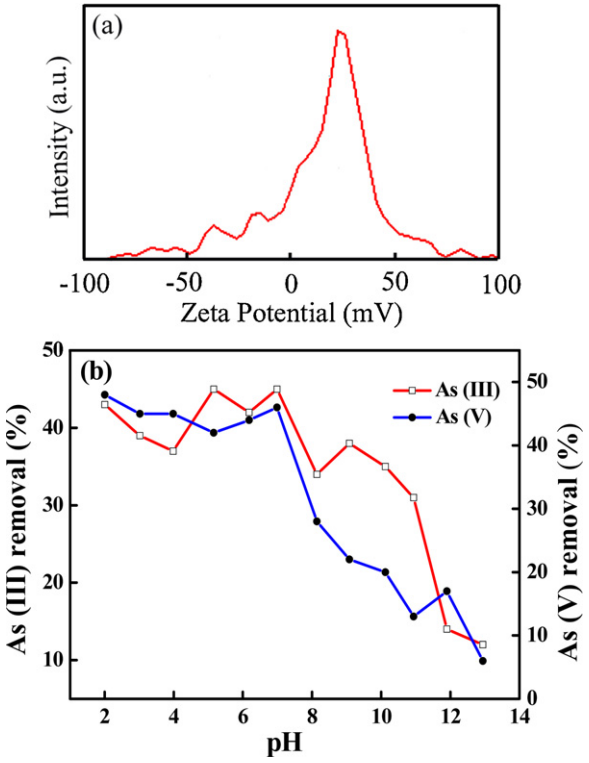


**Fig. 7.** (a) Zeta potential of ascorbic acid-coated $Fe_3O_4$ nanoparticles in an aqueous solution at pH = 7, (b) the influence of pH on As (III) and As (V) adsorption efficiency (%) from stock solution (adsorbent concentration: 60 mg/L, contact time: 24 h).

**Table 1**
the pH values of water before and after the removal of arsenic.

| | | 1 | 2 | 3 | 4 | 5 | 6 | 7 | 8 | 9 | 10 |
|---|---|---|---|---|---|---|---|---|---|---|---|
| As(III) pH | Before | 2.01 | 3.02 | 5.16 | 6.99 | 8.14 | 9.08 | 10.12 | 10.94 | 11.90 | 12.94 |
| | After | 2.32 | 3.4 | 5.41 | 8.79 | 8.84 | 8.98 | 9.25 | 9.69 | 11.54 | 12.88 |
| As(V) pH | Before | 2.06 | 3.01 | 5.04 | 6.93 | 7.94 | 9.07 | 10.01 | 11.04 | 11.97 | 13.02 |
| | After | 2.26 | 3.13 | 5.18 | 7.97 | 8.11 | 8.44 | 9.81 | 10.74 | 11.74 | 12.94 |

potential measurement could provide an important criterion for us to choose harmful compounds to be adsorbed. The sample to be measured was prepared by directly dispersing the ascorbic acid-coated $Fe_3O_4$ nanoparticles in deionized water to form a homogeneous solution and the pH value of this solution is about 7. As shown in Fig. 7a, the zeta potential of the sample is about 24 mV, which indicates that the surface of the ascorbic acid-coated $Fe_3O_4$ nanoparticles is positively charged. This result also suggests that this materials can be used a potential adsorbent for the removal for the metal negative ions. As we know, arsenic(III) and arsenic(V) generally exist in aqueous solution as $AsO_3^{3-}$ and $AsO_4^{3-}$, respectively. Therefore, we used the synthesized ascorbic acid-coated $Fe_3O_4$ nanoparticles to investigate their application for the removal of arsenic. To the best of our knowledge, among all the naturally occurring groundwater contaminants, arsenic is by far the most toxic, and thus its efficient removal from water is of great significance. In addition, the unique advantage of the as-synthesized ascorbic acid-coated $Fe_3O_4$ nanoparticles with the functionality of dehydroascorbic acid for water treatment is that on the one hand, they are hydrophilic and can be well dispersed in water solution, and on the other hand, they can be separated from water by using a magnet (Fig. 5d). While the $Fe_3O_4$ particles obtained without ascorbic acid are non-soluble in water solution.

For water treatment, it is well known that any strategy to remove arsenic from groundwater must take into consideration safe containment of the arsenic removed with no adverse ecological impact. So, we first investigated the pH change of the wastewater before and after the removal of arsenic. Batch adsorption tests were carried out with As(III) and As(V) stock solution (1.0 mg/L) and 60 mg/L of adsorbent. As shown in Table 1, the pH value keeps almost constant before and after the removal of arsenic, indicating that $Fe_3O_4$ adsorbent has no effect on the water quality. This feature is particularly important for the purifying of drinking water.

It has been addressed in the references that the sorption behavior of arsenic is strongly influenced by the pH value of solution [1,26]. So, in our experiments, we first investigated the effect of pH value on arsenic(III) and arsenic(V) removal capacity by the ascorbic acid-coated $Fe_3O_4$ nanoparticles, where the experiments were achieved at different pH values in the range of 2–13 for same contact time of 24 h. Fig. 7b clearly shows that in the acidic pH range of 2–7, both arsenic(III) and arsenic(V) adsorption by the ascorbic acid-coated $Fe_3O_4$ nanoparticles are not significantly affected by pH value, and the removal percentage of arsenic(III) and arsenic(V) basically remains constant at 45%. But when pH is adjusted to higher than 7, the removal percentage of arsenic(III) and arsenic(V) drops sharply less than 15%, which is similar to the result of arsenic removal by mixed magnetite-maghemite [26]. This result indicates that the ascorbic acid-coated $Fe_3O_4$ nanoparticles can remove arsenic(III) and arsenic(V) more readily in an acidic pH range. The amount of arsenic(III) and arsenic(V) uptake both decreased with increasing pH, which may be attributed to zeta potential change of the ascorbic acid-coated $Fe_3O_4$ nanoparticle solution at different pH values. The zeta potentials of the ascorbic acid-coated $Fe_3O_4$ nanoparticle solution at 2, 5, 8, and 12 of pH values are shown in Fig. 8. It can be clearly seen that the zeta potential of the ascorbic acid-coated $Fe_3O_4$ nanoparticle solution gradually changes from positive at a low pH value to negative at a high pH value. Therefore, in the pH range of 2–7, ascorbic acid-coated $Fe_3O_4$ nanoparticles could adsorb negatively charged arsenic(III) and arsenic(V), while

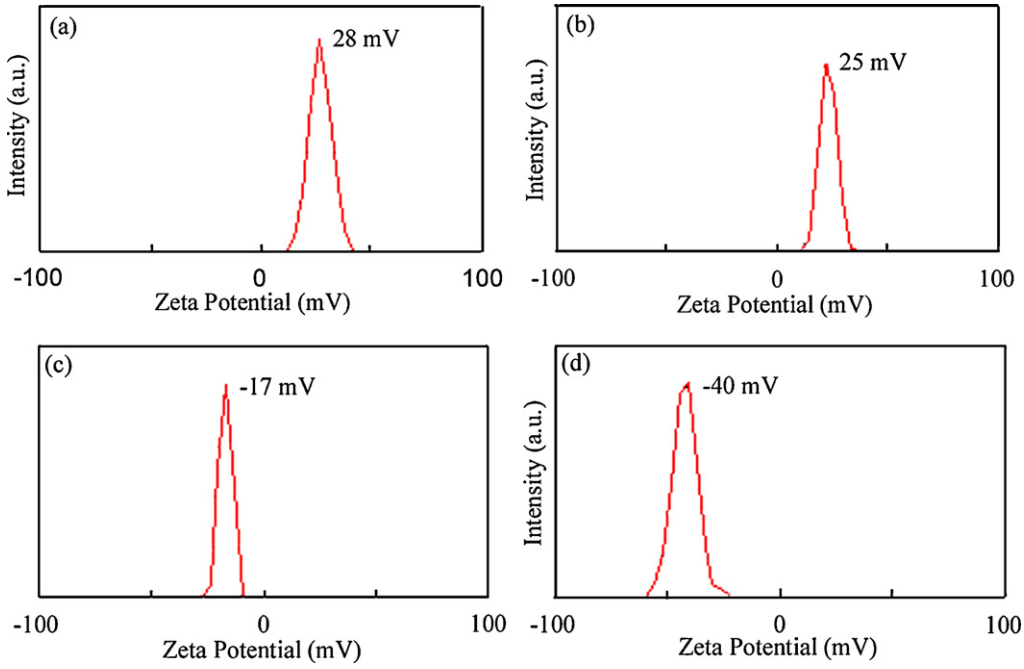


**Fig. 8.** Zeta potential of ascorbic acid-coated $Fe_3O_4$ nanoparticles in aqueous solution at different pH values (a) 2, (b) 5, (c) 8, (d) 12.

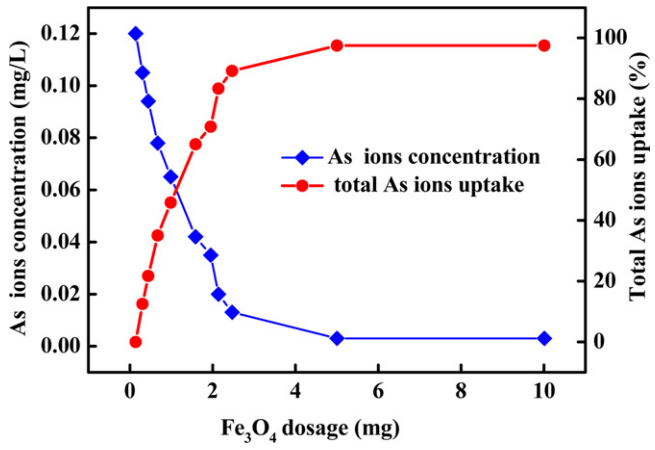


**Fig. 9.** The effect of ascorbic acid-coated $Fe_3O_4$ nanoparticle adsorbent dosage on adsorption of total arsenic ions.

in the pH range of 8–12 they are not favorable adsorbed since they are negatively charged. This result is well agreement with that reported by Hu et al. [10].

Second, we tested the effect of absorbent concentration on arsenic(III) and arsenic(V) removal capacity. The absorption of arsenic at different absorbent concentrations is shown in Fig. 9. In this test, the total concentration of arsenic aqueous solution was kept at 0.12 mg/L. Fig. 9 clearly discloses that the removal efficiency of arsenic increases with the increase of the ascorbic acid-coated $Fe_3O_4$ nanoparticle concentration. The percentage of the removal increases markedly from 12.5% to 97.5% by increasing the concentration the ascorbic acid-coated $Fe_3O_4$ adsorbent from 5.67 to 200.13 mg/L. Actually, the arsenic equilibrium concentration drops to well below 0.042 mg/L at the absorbent concentration of 60 mg/L. Finally, the effect of contact time on arsenic adsorption was also investigated. 25 mL of 0.1 mg/L arsenic solution and 60 mg/L of the ascorbic acid-coated $Fe_3O_4$ nanoparticles were mixed at pH = 7. The effect of contact time on uptake of arsenic ion is shown in Fig. 10. It can be clearly seen that for both cases, the removal mainly includes arsenic rapid uptake within 0.5 h of contact time and slower one, in which the rapid process may be attributed to the external surface adsorption. In addition, the removal efficiency of As(III) is higher than that of As(V) at same initial arsenic concentration of 0.1 mg/L. About 50% of the arsenic (III) was removed during the initial 0.5 h of the adsorption process, but for arsenic (V) only 30% was removed

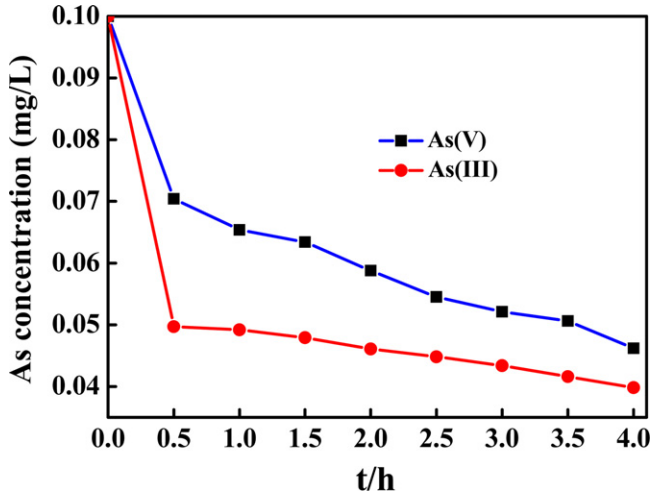


**Fig. 10.** The effect of contact time on the removal of As (III) and As (V) by the ascorbic acid-coated $Fe_3O_4$ nanoparticle.

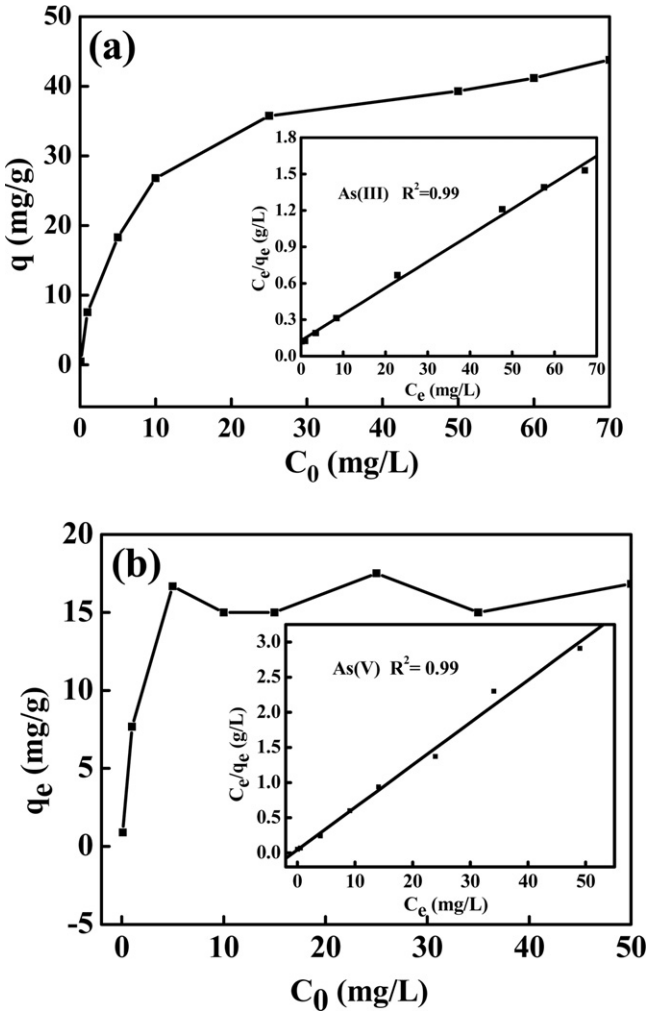


**Fig. 11.** Equilibrium isotherm for the adsorption of As(III) ions (a) and As(V) (b) on the ascorbic acid-coated $Fe_3O_4$ nanoparticles at pH 5 and 300 K (fitted by linearized Langmuir isotherm).

within same time. The reason may be probably due to their different charges.

The adsorption equilibrium isotherms for the adsorption of arsenic(III) and arsenic(V) at pH = 7 and 300 K are shown in Fig. 11, respectively, where adsorbent concentration of 60 mg/L was used. The adsorption data were fitted according to the linear form of the Langmuir adsorption equation as following [8,27]:

Where $C_e$ is As ions equilibrium concentration in solution, $q$ is the adsorption capacity based on the dry weight of nano-adsorbent, $q_m$ is the maximum adsorption capacity, and $K$ is the Langmuir adsorption equilibrium constant. The plot of $C_e/q$ vs $C_e$ at various initial As ion concentrations yielded straight lines, revealing that the adsorption of As ions follows the Langmuir adsorption equation. From the slope and intercept, the values of $q_m$ and $K$ might be estimated to 46.06 mg/g and 0.1686 $Lmg^{-1}$ for As(III), 16.56 mg/g and 1.42 $Lmg^{-1}$ for As(V), respectively, which are better than the reported results of magnetite-maghemite nanoparticles for arsenic adsorption [26]. The difference for As(III) and As(V) adsorption may be probably due to that the adsorption free energy of As(III) ions is lower than that of As(V) ions [26].

As we know, the leaching of sorbent components into the treated water is unfavorable, although ascorbic acid-coated $Fe_3O_4$ is nontoxic. We measured leaching of the synthesized ascorbic acid-coated $Fe_3O_4$ nanoparticles with different concentrations in As(III) aqueous solution of 0.12 mg/L (PH = 7.0). As shown in Table 2, for all

**Table 2**
Leaching of Fe after suspending different concentrations of ascorbic acid-coated $Fe_3O_4$ in As(III) aqueous solution of 0.12 mg/L.

| | 1 | 2 | 3 | 4 | 5 | 6 | 7 | 8 | 9 |
|---|---|---|---|---|---|---|---|---|---|
| Added ascorbic acid-coated $Fe_3O_4$ (mg/L) | 5.67 | 12.29 | 17.95 | 26.85 | 39.53 | 63.54 | 98.82 | 110.34 | 157.68 |
| Leached $Fe^{3+}$ concentration (mg/L) | 0.01 | 0.056 | 0.021 | 0.046 | 0.066 | 0.072 | 0.033 | 0.017 | 0.014 |

cases the concentrations of Fe ions are less than 0.1 mg/L, in which the concentration of Fe ions was measured by Inductively-coupled plasma spectrometer (ICP). Such a low leaching concentration of Fe ions indicates the high stability of the ascorbic acid-coated $Fe_3O_4$ nanoparticles.

## 4. Conclusion

In summary, we presented a simple, environmentally friendly hydrothermal method to obtain superparamagnetic high-surface-area $Fe_3O_4$ nanoparticles. The use of the ascorbic acid not only improves the dispersability of $Fe_3O_4$ nanoparticles in aqueous suspensions, but also effectively inhibits the leaching of Fe into the solution. The prepared $Fe_3O_4$ nanomaterials showed an excellent ability to remove heavy metal arsenic ions in water. The application of $Fe_3O_4$ nanoparticles for heavy metal removal has a great potential in waste water engineering.

## Acknowledgements

This work was supported by the Natural Science Foundation of China (NSFC, Nos. 20731002, 20871016, 10876002, 91022006 and 20973023), the 111 Project (B07012), Program for New Century Excellent Talents in University, Specialized Research Fund for the Doctoral Program of Higher Education (SRFDP, No. 200800070015 and 20101101110031), Funding Project for Science and Technology Program of Beijing Municipal Commission (No. Z09010300820902). We thank Prof. Chuanbi Li for helpful measurements. Special thanks are given to support by key Laboratory of Functional Materials Physics and Chemistry (Jilin Normal University) and Center of Analysis and Testing of Beihua University.

## References

[1] K.P. Raven, A. Jain, R.H. Loeppert, Arsenite and arsenate adsorption on ferrihydrite: kinetics, equilibrium, and adsorption envelopes, Environ. Sci. Technol. 32 (1998) 344–349.
[2] J.F. Ferguson, J. Gavis, A review of the arsenic cycle in natural waters, Water Res. 6 (1972) 1259–1274.
[3] N.E. Korte, Q. Fernando, A review of arsenic(III) in groundwater, Crit. Rev. Environ. Control 21 (1991) 1–39.
[4] V. Chandra, J. Park, Y. Chun, J.W. Lee, In-Ch. Hwang, K.S. Kim, Water-dispersible magnetite-reduced graphene oxide composites for arsenic removal, ACS Nano 4 (2010) 3979–3986.
[5] S. Sarkar, L.M. Blaney, A. Gupta, D. Ghosh, A.K.S. Gupta, Arsenic removal from groundwater and its safe containment in a rural environment: validation of a sustainable approach, Environ. Sci. Technol. 42 (2008) 4268–4273.
[6] C.T. Yavuz, J.T. Mayo, W.W. Yu, A. Prakash, J.C. Falkner, S.J. Yean, L.L. Cong, H.J. Shipley, A. Kan, M. Tomson, D. Natelson, V.L. Colvin, Low-field magnetic separation of monodisperse $Fe_3O_4$ nanocrystals, Science 314 (2006) 964–967.
[7] W. Yantasee, C. Warner, T. Sangvainch, R. Sh Addlemen, T. Carter, R.J. Wiacek, G.E. Fryxell, Ch Timahalk, M.G. Warner, Removal of heavy metals from aqueous systems with thiol functionalized superparamagnetic nanoparticles, Environ. Sci. Technol. 41 (2007) 5114–5119.
[8] Y.C. Chang, D.H. Chen, Preparation and adsorption properties of monodisperse chitosan-bound $Fe_3O_4$ magnetic nanoparticles for removal of Cu(II) ions, J.Colloid Interface Sci. 283 (2005) 446–451.
[9] J.F. Liu, Z.S. Zhao, G.B. Jiang, Coating $Fe_3O_4$ magnetic nanoparticles with humic acid for high efficient removal of heavy metals in water, Environ. Sci. Technol. 42 (2008) 6949–6954.
[10] J. Hu, I.M.C. Lo, G. Chen, Removal of Cr(VI) by magnetite nanoparticle, Water Sci. Technol. 50 (2004) 139–146.
[11] P. Yuan, D. Liu, M.D. Fan, D. Yang, R.L. Zhu, F. Ge, J.X. Zhu, H.P. He, Removal of hexavalent chromium [Cr(VI)] from aqueous solutions by the diatomite-supported/unsupported magnetite nanoparticles, J. Hazard. Mater. 173 (2010) 614–621.
[12] J.P. Jolivet, C. Chaneac, E. Tronc, Iron oxides chemistry. From molecular clusters to extended solid networks, Chem. Commun. (2004) 481–487.
[13] X. Li, X. Yu, J.H. He, Z. Xu, Controllable fabrication, growth mechanisms, and photocatalytic properties of hematite hollow spindles, J. Phys. Chem. C 113 (2009) 2837–2845.
[14] X. Liang, X. Wang, J. Zhuang, Y.T. Chen, D.S. Wang, Y.D. Li, Synthesis of nearly monodisperse iron oxide and oxyhydroxide nanocrystals, Adv. Funct. Mater. 16 (2006) 1805–1813.
[15] H.P. Klug, L.E. Alexander, X-ray Diffraction Procedures for Polycrystalline and Amorphous Materials, John Wiley & Sons, New York, 1962, pp. 491–538.
[16] D.L.A. de Faria, S.V. Silva, M.T. de Oliveira, Raman microspectroscopy of some iron oxides and oxyhydroxides, J. Raman Spectrosc. 28 (1997) 873–878.
[17] U. Schwertmann, R.M. Cornell, Iron Oxides in the Laboratory—Preparation and Characterization, 2nd ed., Wiley-VCH, Weinheim, Germany, 2000, Chapter 1.
[18] Z. Li, W. Li, M.Y. Gao, H. Lei, One-pot reaction to synthesize biocompatible magnetite nanoparticles, Adv. Mater. 17 (2005) 1001–1005.
[19] H.D. Moya, N. Coichev, Kinetic studies of the oxidation of L-ascorbic acid by tris(oxalate)cobaltate in the presence of CDTA metal ion complexes, J. Braz. Chem. Soc. 17 (2006) 364–368.
[20] B.L. Cushing, V.L. Kolesnichenko, C.J. O'Connor, Recent advances in the liquid-phase synthesis of inorganic nanoparticles, Chem. Rev. 104 (2004) 3893–3946.
[21] X.H. Sun, C.M. Zheng, F.X. Zhang, Y.L. Yang, G.J. Wu, A.M. Yu, N.J. Guan, Size-controlled synthesis of magnetite ($Fe_3O_4$) nanoparticles coated with glucose and gluconic acid from a single Fe(III) precursor by a sucrose bifunctional hydrothermal method, J. Phys. Chem. C 113 (2009) 16002–16008.
[22] Z. Li, Q. Sun, M.Y. Gao, Preparation of water-soluble magnetite nanocrystals from hydrated ferric salts in 2-pyrrolidone: mechanism leading to $Fe_3O_4$, Angew. Chem. Int. Ed. 44 (2005) 123–126.
[23] X.H. Sun, C.M. Zheng, F.X. Zhang, L.D. Li, Y.L. Yang, G.J. Wu, N.J. Guan, β-cyclodextrin-assisted synthesis of superparamagnetic magnetite nanoparticles from a single Fe(III) precursor, J. Phys. Chem. C 112 (2008) 17148–17155.
[24] M.P. Morales, S. Veintemillas-Verdaguer, M.I. Montero, C.J. Serna, A. Roig, L. Casas, B. Martinez, F. Sandiumenge, Surface and internal spin canting in (-$Fe_2O_3$ nanoparticles, Chem. Mater. 11 (1999) 3058–3064.
[25] Z. Li, B. Tan, M. Allix, A.I. Cooper, M.J. Rosseinsky, Direct coprecipitation route to monodisperse dual-functionalized magnetic iron oxide nanocrystals without size selection, Small 4 (2008) 231–239.
[26] S.R. Chowdhury, E.K. Yanfu, Arsenic and chromium removal by mixed magnetite maghemite nanoparticles and the effect of phosphate on removal, J. Environ. Manage. 91 (2010) 2238–2247.
[27] W.S.W. Ngah, C.S. Endud, R. Mayanar, React. Funct. Polym. 50 (2002) 181–190.